

Beat-frequency adjustable Er³⁺-doped DBR fiber laser for ultrasound detection

Tuan Guo,^{1,2,*} Allan C. L. Wong,³ Wei-Sheng Liu,¹ Bai-Ou Guan,²
Chao Lu,³ and Hwa-Yaw Tam¹

¹ Photonics Research Center, Department of Electrical Engineering, The Hong Kong Polytechnic University, Kowloon, Hong Kong SAR, China

² Institute of Photonics Technology, Jinan University, Guangzhou 510632, China

³ Photonics Research Center, Department of Electronic and Information Engineering, The Hong Kong Polytechnic University, Kowloon, Hong Kong SAR, China

*tuanguo@jnu.edu.cn

Abstract: A compact low beat-frequency dual-polarization distributed Bragg reflector (DBR) fiber laser whose beat frequency can be varied, for high-frequency ultrasound detection has been proposed and experimentally demonstrated. The laser was fabricated in small birefringent commercial erbium-doped fiber. It operated in a robust single-longitude mode with output power of more than 1 mW and high signal-to-noise ratio better than 60 dB. Induced birefringence to the fiber during the UV inscription process is small ($\sim 10^{-7}$) and consequently the laser beats at a low frequency of ~ 20 MHz which is at least one order of magnitude smaller than previously reported results, making frequency down-conversion unnecessary. The beat frequency can be adjusted by controlling the side-exposure time of the UV light irradiating the gain cavity, providing a simple approach to multiplex a large number of DBR fiber lasers of different frequencies in series using frequency division multiplexing (FDM) technique. The proposed DBR fiber laser is also temperature insensitive, making it a good candidate for hydrophone applications.

©2011 Optical Society of America

OCIS codes: (060.2370) Fiber optics sensors; (060.0060) Fiber optics and optical communications.

References and links

1. H. K. Kim, S. K. Kim, H. G. Park, and B. Y. Kim, "Polarimetric fiber laser sensors," *Opt. Lett.* **18**(4), 317–319 (1993).
2. G. A. Ball, G. Meltz, and W. W. Morey, "Polarimetric heterodyning Bragg-grating fiber-laser sensor," *Opt. Lett.* **18**(22), 1976–1978 (1993).
3. K. P. Koo, and A. D. Kersey, "Bragg grating-based laser sensors systems with interferometric interrogation and wavelength division multiplexing," *J. Lightwave Technol.* **13**(7), 1243–1249 (1995).
4. J. T. Kringlebotn, W. H. Loh, and R. I. Laming, "Polarimetric Er(3+)-doped fiber distributed-feedback laser sensor for differential pressure and force measurements," *Opt. Lett.* **21**(22), 1869–1871 (1996).
5. Y. Zhang, B. O. Guan, and H. Y. Tam, "Characteristics of the distributed Bragg reflector fiber laser sensor for lateral force measurement," *Opt. Commun.* **281**(18), 4619–4622 (2008).
6. O. Hadeler, E. Rønnekleiv, M. Ibsen, and R. I. Laming, "Polarimetric distributed feedback fiber laser sensor for simultaneous strain and temperature measurements," *Appl. Opt.* **38**(10), 1953–1958 (1999).
7. D. J. Hill, P. J. Nash, D. A. Jackson, D. J. Webb, S. F. O'Neill, I. Bennion, and L. Zhang, "A fibre laser hydrophone array," *Proc. SPIE* **3860**, 55–66 (1999).
8. S. W. Løvseth, J. T. Kringlebotn, E. Rønnekleiv, and K. Bløtekjaer, "Fiber distributed-feedback lasers used as acoustic sensors in air," *Appl. Opt.* **38**(22), 4821–4830 (1999).
9. K. Bohnert, A. Frank, E. Rochat, K. Haroud, and H. Brändle, "Polarimetric fiber laser sensor for hydrostatic pressure," *Appl. Opt.* **43**(1), 41–48 (2004).
10. B. O. Guan, H. Y. Tam, S. T. Lau, and H. L. W. Chan, "Ultrasonic hydrophone based on fiber distributed Bragg reflector laser," *IEEE Photon. Technol. Lett.* **17**(1), 169–171 (2005).
11. S. Foster, A. Tikhomirova, M. Englund, H. Inglis, G. Edvells, and M. Milnes, "A 16 channel fibre laser sensor array," *ACOFT/AOS* 10–13 (2006).
12. Y. Jiang, "Wavelength division multiplexing addressed four-element fiber optical laser hydrophone array," *Appl. Opt.* **46**(15), 2939–2948 (2007).

13. L. Y. Shao, S. T. Lau, X. Y. Dong, A. P. Zhang, H. L. W. Chan, H. Y. Tam, and S. L. He, "High-frequency ultrasonic hydrophone based on a cladding-etched DBR fiber laser," *IEEE Photon. Technol. Lett.* **20**(8), 548–550 (2008).
 14. B. O. Guan, Y. N. Tan, and H. Y. Tam, "Dual polarization fiber grating laser hydrophone," *Opt. Express* **17**(22), 19544–19550 (2009).
 15. L. Flax, J. H. Cole, R. P. De Paula, and J. A. Bucaro, "Acoustically induced birefringence in optical fibers," *J. Opt. Soc. Am.* **72**(9), 1159–1162 (1982).
 16. W. H. Loh, L. Dong, and J. E. Caplen, "Single-sided output Sn/Er/Yb distributed feedback fiber laser," *Appl. Phys. Lett.* **69**(15), 2151–2153 (1996).
 17. J. Q. Sun, J. L. Qiu, and D. X. Huang, "Multiwavelength erbium-doped fiber lasers exploiting polarization hole burning," *Opt. Commun.* **182**(1-3), 193–197 (2000).
 18. J. J. Zayhowski, "Limits imposed by spatial hole burning on the single-mode operation of standing-wave laser cavities," *Opt. Lett.* **15**(8), 431–433 (1990).
 19. H. L. W. Chan, K. S. Chiang, D. C. Price, and J. L. Gardner, "The characterization of high-frequency ultrasonic fields using a polarimetric optical fiber sensor," *J. Appl. Phys.* **66**(4), 1565–1570 (1989).
 20. S. C. Rashleigh, "Origins and control of polarization effects in single-mode fibers," *J. Lightwave Technol.* **1**(2), 312–331 (1983).
 21. S. C. Rashleigh, and M. J. Marrone, "Temperature dependence of stress birefringence in an elliptically clad fiber," *Opt. Lett.* **8**(2), 127–129 (1983).
-

1. Introduction

Active, polarimetric sensors based on direct beat-frequency measurement of the two eigen-polarization modes from a distributed Bragg reflector (DBR) fiber laser offer an attractive approach to detect high frequency ultrasound as they benefitted from high sensitivity and the ability of multiplexing a large number of such sensors along a single fiber via wavelength-division multiplexing (WDM) technique [1–3]. In the last two decades, extensive researches have been investigated for high performance DBR fiber sensor applications, including the measurement of transverse pressure [1,4], lateral force & torsion [5,6] and high-frequency ultrasound detection [7–14]. However, the carrier beat signal in these schemes operated at a frequency range from about 1 GHz to several GHz, restricting their practical applications due to the need of a mixer and a local oscillator to down-convert the beat frequency.

In this Letter, we demonstrate the performance of a low beat-frequency single-longitude-mode dual-polarization DBR fiber laser using a commercial erbium-doped fiber which has very low birefringence. The grating-inscription induced a small birefringence at a level of 10^{-7} , producing a stable low beat-frequency as low as 20 MHz. The beat frequency can be easily varied over a relatively large frequency range by controlling the exposure time of the UV-light irradiating the gain cavity, providing a simple approach to multiplex a large number of sensors using frequency division multiplexing (FDM) technique. The low beat frequency features simplified demodulation process. This couples with the sensor's very low temperature sensitivity and multiplexing capability, making such sensor an excellent candidate for low-cost detection of ultrasound.

2. DBR fiber laser design and fabrication

The DBR fiber laser used in the experiment consisted of a pair of wavelength-matched Bragg gratings written in an erbium-doped fiber. Because of the strong directionality of the grating writing process (polarization orientation of the writing beam) and the minor core asymmetry (nonuniformities in the preform fabrication and in fiber drawing), fiber birefringence was generated. The fiber birefringence causes the laser to operate in two orthogonal polarization modes with a small wavelength difference. Consequently, a polarization-mode beat signal at relatively low frequency was generated. When the DBR fiber laser was subjected to an acoustic field, the acoustic pressure changed the fiber refractive index owing to the photoelastic effect. In the case of acoustic wavelength comparable to or smaller than the fiber diameter, the acoustic pressure changes the fiber birefringence due to the different refractive index modulation along and perpendicular to the propagation direction of acoustic wave [15]. Therefore, the polarization mode beat frequency is inherently sensitive to high frequency ultrasonic wave. The frequency and the amplitude of the acoustic pressure could be

determined simultaneously by measuring the frequency and the amplitudes of the upper and lower sidebands of the RF spectrum.

In order to have a small fiber birefringence, the active fiber used in our experiments was a commercial erbium-doped fiber (EDF) (Er-1550C, Corning Ltd), manufactured with outside vapor deposition (OVD) process that offers outstanding consistency and uniformity in the drawn fibers. The EDF has a core diameter of 4.2- μm and its cross-section is shown in Fig. 1. The core-to-cladding offset is less than 0.4 μm and the typical splicing loss of the fiber to SMF-28 optical fiber is 0.1 dB. The fiber has a very small birefringence. The induced core birefringence ($\Delta n = n_{\text{eff}(y)} - n_{\text{eff}(x)}$) is mainly attributed to the UV grating inscription process. The UV-induced birefringence in the smaller core is expected to be much smaller than that in the 16- μm diameter inner cladding of the Er/Yb co-doped fiber reported in [10], resulting in a much lower beat-frequency of the two orthogonal polarizations, and therefore simplifies the demodulation process.

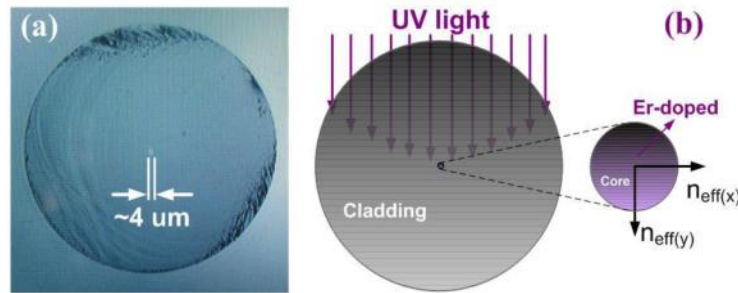


Fig. 1. Photograph of the cross-section of small-core Er-doped active fiber (a) and its induced refractive index modulation under UV-light side-inscription (b).

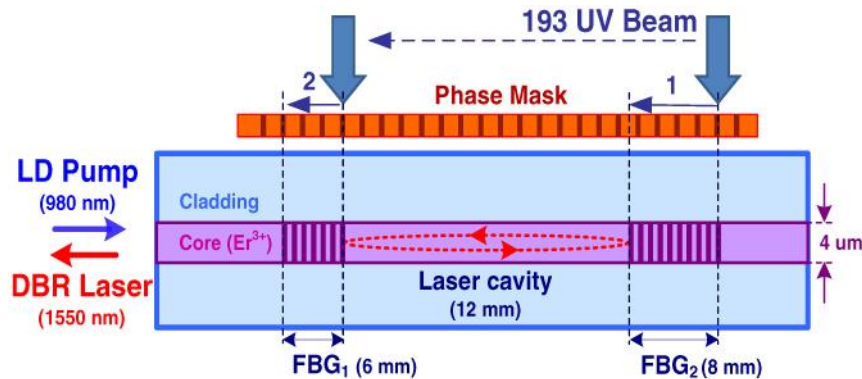


Fig. 2. Schematic diagram and inscription process of an Er-doped DBR fiber laser.

Figure 2 shows the schematic diagram of the short-cavity DBR fiber laser and its inscription process. The DBR laser was fabricated by directly inscribing two wavelength-matched Bragg gratings into a short section of small-core EDF. Because of the small core (4.2- μm) and the very low photosensitivity of the EDF, the commonly used 248 nm KrF excimer laser cannot achieve strong fiber grating inscription in such fiber, even with hydrogen-loading. Thanks to the high efficiency of writing FBGs at 193 nm which is associated with the two-photon excitation process, strong fiber grating inscription over a short section was achieved by using an 193 nm ArF excimer laser for DBR fiber laser fabrication. Hydrogen-loading was therefore not required. This not only simplifies the procedure for laser fabrication but also avoids the laser efficiency degradation arising from the hydrogen loading induced loss at pump wavelength [16]. We use beam scanning technique for the grating fabrication, in which the phase mask and the fiber were fixed, while the laser beam scanned

along the fiber. The two gratings were written with the same beam scanning speed so that they had the same ac and dc index change and thus the same Bragg wavelength.

The energy and repetition rate of the 193 nm excimer laser were set to 100 mJ/cm² and 10 Hz, respectively. We first wrote the high reflectivity (HR) grating. The grating transmission spectrum was monitored by using an Er-doped fiber amplified spontaneous emission (ASE) source and an optical spectrum analyzer (OSA). An 8-mm long HR grating with reflectivity around 99.9% was easily fabricated with our inscription system. We then wrote the low reflectivity (LR) grating using the same beam scanning speed and the same laser settings. During the inscription of the LR grating, the 980 nm LD pump laser was turned on, so the DBR fiber laser output could be monitored. Under the condition that the gain compensating the cavity loss, the laser starts to oscillate when the grating length reaches to ~5 mm. We stopped the grating inscription process after the laser output power slightly exceeded the maximal value and finally got the LR grating with the length of 6 mm. The reflectivity of the LR grating is estimated to be ~90%. Therefore, the total length of the DBR fiber laser is 26 mm, with the lengths of the two FBGs are 6 mm and 8 mm, separated by a 12-mm long gain cavity.

3. Experiment and discussion

The experimental setup of the ultrasound detection system is shown in Fig. 3. The DBR fiber laser was pumped by a 980 nm laser diode (LD) through a 980/1550 nm wavelength division multiplexer (WDM). The DBR laser output was split into two parts by a 3-dB coupler (OC). One output was monitored using an optical spectrum analyzer (OSA, Yokogawa AQ 6370), and the other was injected to a photodetector (PD, Newfocuss 1811-FC, 25 kHz - 125 MHz) which is connected to an electrical spectrum analyzer (ESA, Agilent Technologies E8247C, 250 kHz - 40 GHz). By adjusting the polarization controller (PC) and the polarizer, the beating of the two orthogonal polarization lasing modes can be maximized at the PD. Periodic voltage waveform supplied by a function generator (FG) was used to drive the focused transducer (Panametrics V312) to generate ultrasound in the water. The DBR fiber laser was located at the focused ultrasound field. The water tank was lined with sonic absorbent rubber to avoid reflections from the walls of the water tank.

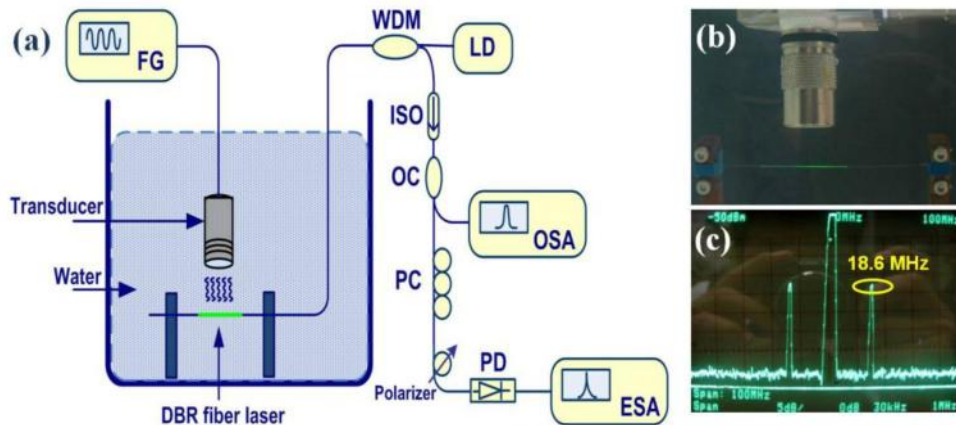


Fig. 3. Schematic diagram of the ultrasound detection system (a) and photographs of an Er-doped DBR fiber laser ultrasound detector (b) and display of the measured spectrum (c).

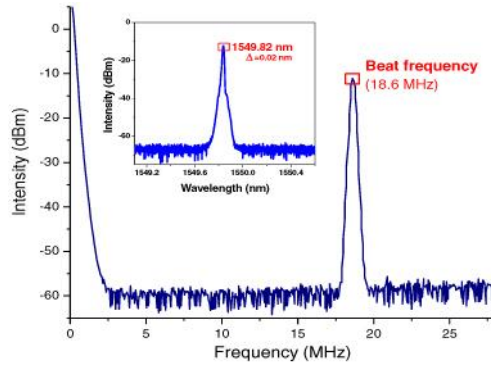


Fig. 4. Beat-signal spectrum of the DBR fiber laser. Insert shows the laser output optical spectrum.

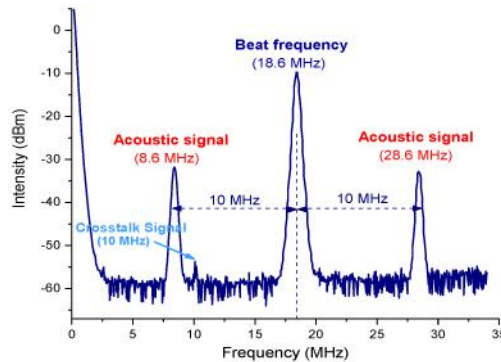


Fig. 5. Beat signal spectrum of DBR fiber laser (18.6 MHz) with an ultrasound of 10 MHz.

Since the dual laser modes are of two linearly orthogonal polarization modes, the polarization hole burning (PHB) effect is enhanced in the cavity [17]. In addition, the round-trip loss of the short linear cavity is relatively low, so a well-defined standing wave will be formed between the two FBGs and thus spatial-hole burning (SHB) occurs [18]. The combination of PHB and SHB effects will reduce the homogeneous linewidth of the EDF and suppress the competition between different modes. Therefore, stable dual orthogonal polarization modes oscillation can be achieved at room temperature. Figure 4 shows the beat signal spectrum recorded by the ESA. The DBR fiber laser operated at a robust single longitude mode with output power of more than 1 mW and signal-to-noise ratio better than 60 dB at OSA resolution of 0.06 nm (as the inset shown in Fig. 4), producing a stable beat signal with a peak-frequency of 18.6 MHz (corresponds to a birefringence of $\Delta n = 1.4 \times 10^{-7}$) and signal-to-noise ratio better than 50 dB (ESA resolution of 10 KHz).

Figure 5 shows the beat signal spectrum when the acoustic transducer was driven at 10 MHz. As expected, the beat signal is frequency modulated (FM) by the acoustic signal and sidebands appeared when the DBR fiber laser was subjected to the ultrasound signal. Since the beat signal can be approximated as a small signal FM modulated signal, the two sidebands follows a linear relationship with the applied ultrasound signal, both in frequency and amplitude (over the input signal range of the transducer), as shown in Fig. 6. Here it should be noted that the amplitude of the sidebands is a function of fiber angular orientation (rotational around its axis) as well as fiber axis pointing orientation (axis is perpendicular to the direction of the ultrasound) relative to the ultrasound source. In the case that an ultrasonic wave is incident normally upon a fiber, the induced change in birefringence is given by [19] $\Delta B = k p_a \sin \omega_a t \cos 2\theta$, where ΔB is the change of the fiber birefringence, k is a constant depending on the acoustic frequency, the photoelastic coefficients and the refractive index of

the optical fiber, p_a and ω_a are the amplitude and angular frequency of the acoustic pressure, respectively, θ is the angle between the polarization axis of the fiber and the propagation direction of the acoustic wave. By measurement of the frequency and the amplitudes, relative to the carrier of the upper and lower sideband components, the frequency and the angular amplitude of the acoustic pressure can be determined simultaneously. The resolution of the ultrasound measurement is limited by the beat frequency drift and the slight amplitude fluctuation of the DBR fiber laser, which was observed to be ~ 50 kHz (beat frequency drift) and 0.1 dB (amplitude fluctuation) in the free-running mode. The maximum detectable ultrasound frequency is limited by the acoustic transducer used in our experiment (specified at an operating frequency of 10 MHz and with the maximum of 16 MHz), while the detectable ultrasound frequency potentially can be increased up to several tens of MHz by monitoring the upper sideband of the RF spectrum combining with an improved sensitivity by reducing the diameter of the DBR laser via wet etching technique [13].

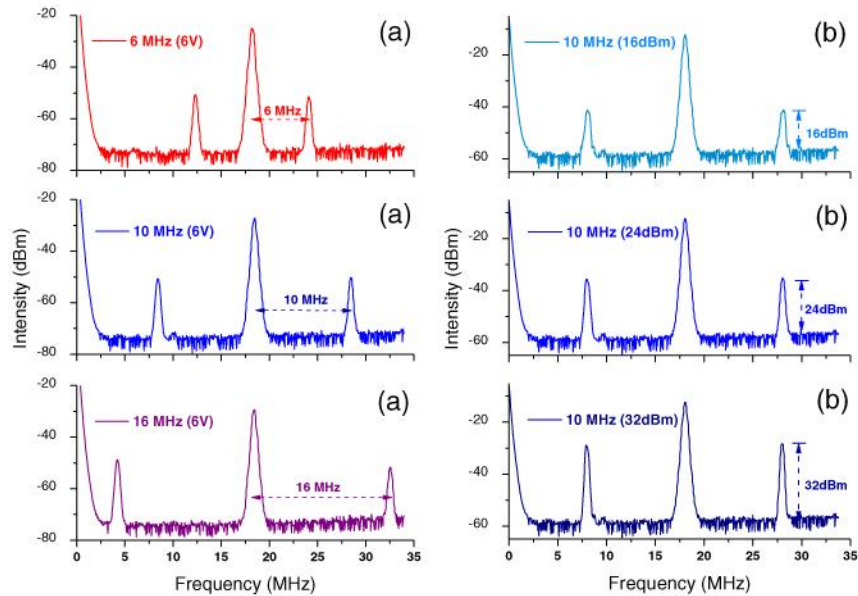


Fig. 6. Beat-signal spectra of the DBR fiber laser versus ultrasounds at different (a) frequencies and (b) amplitudes.

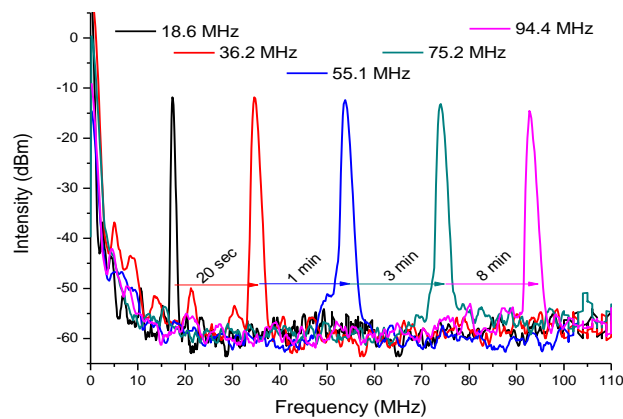


Fig. 7. Beat-frequency of the DBR fiber laser by irradiating the gain cavity of the DBR laser with different UV-light exposure times.

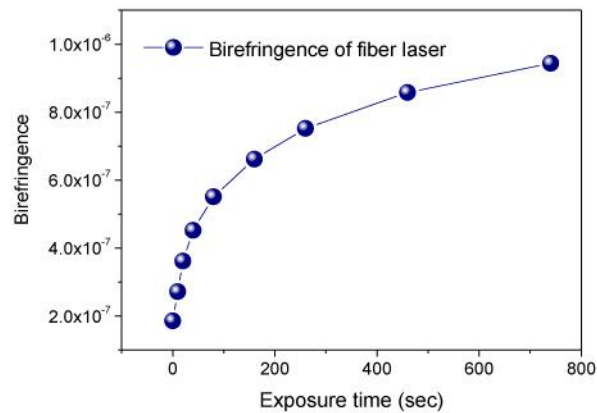


Fig. 8. Birefringence of the gain cavity of the DBR fiber laser versus UV-light exposure time.

A unique advantage of the DBR fiber laser is the ease of varying its beat-frequency by adjusting the amount of UV-light irradiating the gain cavity (i.e., excluding the grating section on either side). After the DBR fiber has been fabricated as described above, it was left on the fiber holders with the phase mask removed, and the UV beam was scanned along the fiber laser gain cavity (i.e. the 12-mm region between the two gratings as shown in Fig. 2). EDF has high germanium concentration and direct UV-light exposure will induce an increase in refractive index along the fiber core but not uniformly across its cross-section. The region of the fiber core facing the UV-beam (please see Fig. 1) will receive a slightly higher dose of UV-fluences than the region on the opposite side. The UV-light irradiated the gain cavity and the gratings at different times but on the same side of the fiber and thus the laser's birefringence can be further increased even after it was fabricated. Consequently, the beat frequency of the DBR laser can be increased by increasing the UV dosage to the laser's gain cavity. Figure 7 shows the superimposed spectra of the polarization beat signals of the DBR fiber laser for different UV-light exposure times and Fig. 8 presents the exact relationship between the modulated laser's birefringence and the UV-light exposure time. Note that the change in beat frequency (or birefringence of fiber laser) has a nonlinear relationship with the UV exposure time - the rate of increase in the beat frequency decreases with exposure time. In our case, we observed that the saturation occurred after about 10 minutes, as shown in Fig. 8. This is due to saturation in the refractive index change in the fiber core, which restricts the nonuniformity in the refractive index across the cross-section of the fiber core that the UV light can induce, and hence limits the maximum value of the beat frequency. If desired, the maximum beat-frequency of the DBR laser could be increased by hydrogen-loading of the EDF to make it more photosensitive. This unique feature of adjusting the beat-frequency allows the DBR fiber laser to be used to detect ultrasound of higher frequency by directly monitoring the lower sideband of the RF spectrum, allowing inexpensive photodetectors and low-speed electronics to be used to demodulate the sensing signals. Also, it provides a simple approach to multiplex a large number of DFB fiber lasers at different frequencies by FDM technique. This provides another dimension of sensor multiplexing in addition to WDM multiplexing.

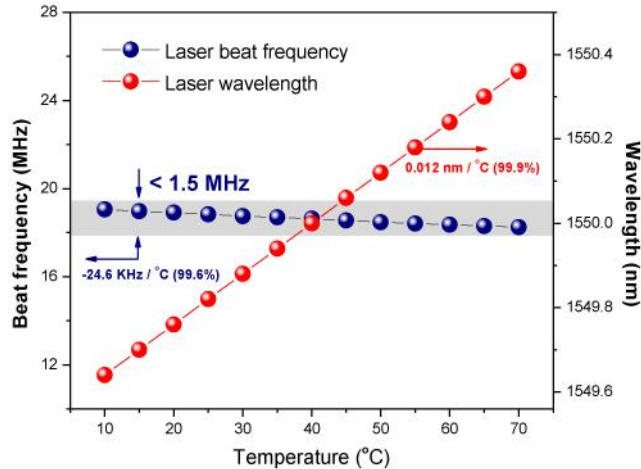


Fig. 9. Beat signal spectra versus temperature.

The temperature-insensitive feature of the DBR fiber laser is demonstrated in Fig. 9. For a temperature change from 10 °C to 70 °C, the carrier beat frequency shifts by less than 1.5 MHz, with a linear response of -24.6 kHz/°C, which is significantly lower than early reported results of $\sim 10^3$ kHz/°C [7–14]. This characteristic is very useful for practical applications where temperature change is not too large and thus temperature effect can be ignored. The slightly negative change in beat frequency with increasing temperature is believed to be the result of stress relaxation of UV-inscribed birefringence along the gratings and the inherent residual stress of the Er-doped gain cavity [20,21], which shows a reversible property in repeat temperature tests and is hard to remove by heat treatment. The laser output wavelength shifted with temperature at a rate of 12 pm/°C, same as conventional FBGs.

4. Conclusions

We have demonstrated a dual-polarization DBR fiber laser fabricated in commercial EDF that was capable of detecting ultrasound with frequency up to 16 MHz. The laser operated in robust single mode with output power more than 1 mW and signal-to-noise ratio better than 60 dB. The small core coupled with the small birefringence fiber design resulted in the proposed ultrasonic sensor with the following desirable features: (i) low beat frequency of about 20 MHz that is much lower than ~ 1 GHz reported previously. This is important because it greatly simplified the demodulation scheme, (ii) very small temperature sensitivity and therefore temperature compensation can be avoided in most practical applications, (iii) compact size, (iv) tunable beat frequency to tailor for different applications, and (v) multiplexing capability that provide a simple approach to multiplex large number of sensing points via FDM and WDM techniques.

Acknowledgments

The authors acknowledge support by grants from The Hong Kong Polytechnic University of Hong Kong Special Administrative Region, China (Project No. G-YX0W), the RGC General Research Fund of the Hong Kong Government (Project No. PolyU 5281/08) and the Key Project of National Natural Science Foundation of China (60736039). The authors also wish to thank Mr. Hongjun Wang and Miss Da Chen for fabricating the DBR lasers.